

## Real-Time Simultaneous Wide- and Small-Angle Fibre Diffraction

W. Bras,<sup>a,b</sup> G. R. Mant,<sup>a</sup> G. E. Derbyshire,<sup>a</sup> W. J. O’Kane,<sup>c</sup> W. I. Helsby,<sup>a</sup>  
C. J. Hall<sup>a</sup> and A. J. Ryan<sup>c,a\*</sup>

<sup>a</sup>Daresbury Laboratory, Warrington WA4 4AD, UK, <sup>b</sup>Netherlands Organisation for Scientific Research (NWO), The Hague, The Netherlands, and <sup>c</sup>Manchester Materials Science Centre, UMIST, Manchester M1 7HS, UK

(Received 31 October 1994; accepted 16 December 1994)

A combination of two independent imaging area-detector systems controlled by a single data-acquisition system, provides a powerful system for X-ray diffraction studies of time-resolved phenomena over a wide  $q$  range, in samples with intrinsic or induced structural orientation. With this system we have observed a transient, tensile-stress-induced, orthorhombic-to-monoclinic transition in high-density polyethylene.

**Keywords:** simultaneous recording; SAXS; WAXS; phase transitions; fibre diffraction; polyethylene.

### 1. Introduction

There are undeniable advantages in performing simultaneous experiments when studying the time evolution of structure in samples subjected to an external driving force. Not only is it that any possible discrepancy is eliminated between results due to different sample preparations, but also systematic errors such as, for example, differences in sample temperature or stress levels between two independent experiments, are removed. This is especially important when transient phenomena are studied. In order to perform time-resolved X-ray experiments, a very bright X-ray source is needed which limits this type of experiment to the domain of synchrotron radiation laboratories in all but the slowest time scale ( $> 20$  min/data set).

Recently, we have reported on equipment assembled to perform small-angle X-ray scattering (SAXS) and wide-angle X-ray scattering (WAXS) simultaneously (Bras *et al.*, 1993). However, the combination of linear detectors used in that system makes the system less useful when dealing with samples exhibiting anisotropy in the scattering pattern. In order to obtain the full information contained in the X-ray diffraction pattern of such samples, it is essential to use detectors which will yield two-dimensional diffraction information. This imposes rather challenging problems if one wants to study systems in which information over large  $q$  ranges has to be assessed simultaneously and with a fine time resolution.

A number of attempts to solve this experimental problem have been made so far. The first is to utilize a synchrotron beamline with an extremely good collimation in combination with a detector with a high spatial resolution. The problem with this solution is twofold. First, the collimation

has to be extremely good, which limits the applicability to third-generation synchrotron radiation sources. Second, the small-angle pattern will be mapped onto a very small number of pixels of the detector unless an extremely large detector is used. Detectors with large active areas in use at the moment are gas-filled proportional wire chambers (GFPWC) which do not have the extremely good spatial resolution required for this technique and, moreover, exhibit parallax problems for wider scattering angles (Hall & Lewis, 1994).

A second solution is the method adopted by Bark, Schulze & Zachmann (1990), in which the combination of a fluorescent screen and a video camera is used to follow the time evolution of the wide-angle pattern. A hole in the fluorescent screen allows the small-angle region to be detected by a GFPWC detector. The limited dynamic range of the fluorescent screen necessitates that the wide-angle pattern subsequently has to be re-recorded with an area detector in an independent experiment optimized for wide-angle data collection, in order to obtain quantitative data. By using the wide-angle data obtained in the first experiment for time registration, an accurate time correlation between the experiments is established. However, the advantages of performing experiments on one single sample are lost. Another limitation of this system is that the time resolution is low ( $> 30$  s/data frame).

A third solution consists of translating a set of X-ray films or image plates, with an appropriate hole to allow the small-angle pattern through, across the X-ray beam path. This has to be combined with a local shutter which closes during the translation of the films. This obviously allows the recording of high-quality wide-angle diffraction data but is limited in time resolution due to the need to transfer the films mechanically.

\* To whom correspondence should be addressed.

A fourth solution is obviously to utilize two electronic imaging detectors: one to record the small-angle pattern and the other to record part of the wide-angle pattern. Practically, this means that slightly less than one quadrant of the wide-angle pattern can be recorded and that parallax problems will be encountered for the GFPWC. This again will make it difficult to obtain quantitative data from the wide-angle pattern. This method, however, has the potential to obtain time resolution that is only limited by the data rate that the detectors can handle, and by the time framing limitations of the data-acquisition electronics. The latter can be as low as  $10\ \mu\text{s}$  (Mant, 1994).

We have adopted the latter method in our experimental set-up and show that it allows experiments with a sub-second time resolution and an acceptable accuracy.

## 2. Experimental details

Experiments were performed on the SAXS/WAXS beam-line station 8.2 at the SRS in Daresbury. A description of this station has been given elsewhere (Bras *et al.*, 1993) and only the essential details are presented here.

The station produces a highly collimated X-ray beam with a wavelength  $\lambda = 1.52\ \text{\AA}$ . The beam size in the focal plane is approximately  $0.3 \times 3.5\ \text{mm}^2$  and the intensity  $4 \times 10^{10}\ \text{photons s}^{-1}$ . Both the horizontal and vertical divergence angles are low.

For these experiments two identical gas-filled proportional imaging detectors have been used. These detectors have been extensively tested for small-angle diffraction work (Lewis *et al.*, 1988). The active area of both detectors measures  $20 \times 20\ \text{cm}^2$ . The count rate that these detectors can handle is dependent on the nature of the diffraction pattern since local count rate limitations with high intensity peaks have to be applied. An overall count rate of  $8 \times 10^5\ \text{counts s}^{-1}$  is feasible in general. The spatial resolution is approximately  $0.3 \times 0.3\ \text{mm}^2$  at small angles of incidence. This number becomes less favourable at high angles of incidence.

The distance between the sample position and the small-angle detector was set to 370 cm in order to allow the scattering pattern to diverge away from the direct beam and parasitic scatter cone (see Fig. 1). To reduce the air scatter a vacuum chamber was positioned between the sample and the small-angle diffraction (SAD) detector. A beam stop is mounted in this chamber near the SAD detector to prevent the direct beam impinging onto the detector. The entrance window has a diameter of 5 cm and is made of  $60\ \mu\text{m}$  thick Kapton foil. The exit window is constructed out of  $120\ \mu\text{m}$  thick Kapton foil. The SAD detector is generally set to detect a symmetrical pattern but can be offset in order to increase the detectable  $q$  range. The symmetrical position is favoured since this allows any asymmetry in the diffraction, either due to improper mounting of the sample or induced by the sample environment (*e.g.* tensile tester), to be detected.

To circumvent partially the parallax problem of the wide-angle detector, this was mounted at an angle of  $45^\circ$  with respect to the plane of the direct beam, at a distance of 35 cm. This detector can be moved laterally in order to either detect a symmetrical meridional pattern or a one-sided part of a diffraction quadrant. The edge of the detector just clears the SAD pattern. Theoretically the detectable  $q$  range could be improved by lowering this detector so that it would intercept the top half of the SAD pattern, but this only gives a marginal improvement. There is a relatively large air gap between the sample, the wide-angle diffraction (WAD) detector and the entrance to the SAD vacuum chamber. In order to evacuate this space a complicated chamber should be constructed. This would not alleviate all problems due to the inward bulging of the vacuum window before the SAD window. This bulging ( $\approx 7\ \text{cm}$ ) is hardly a problem for the SAD detector where, due to the large distance, it only introduces an error of about 0.5% in the air path length. For the WAD detector this comes to 20% variation over the active area of the detector. A better solution is to insert a helium chamber made from a light frame covered with thin windows ( $25\ \mu\text{m}$  Mylar) in the air path.

The focal plane was positioned between the two detectors. As shown before (Bras *et al.*, 1993), this introduces negligible smearing due to over or under focus in the two detector planes.

The data-acquisition system is capable of time framing at a rate of  $10\ \mu\text{s frame}^{-1}$  with a minimum dead time of  $10\ \mu\text{s}$  between frames. As a result of the count rate limitations of the detectors, however, a more realistic regime is 0.01 s per data-collection frame.

The WAD data-acquisition system used was based upon CAMAC electronics, which have been described elsewhere (Lewis *et al.*, 1988), but controlled by a VME-based computer system comprising Motorola MVME147 processor and CES CAMAC branch driver. The SAD data-acquisition system was completely VME-based and consisted of a

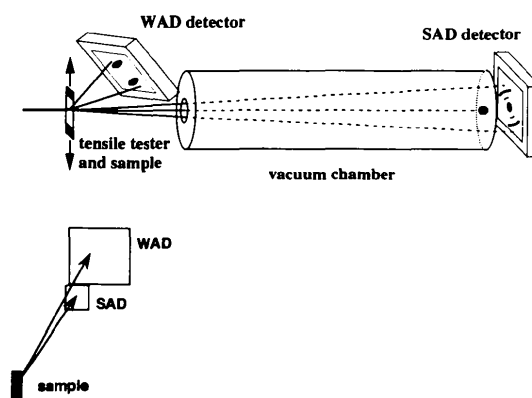


**Figure 1** Schematic drawing of the combined SAD/WAD equipment and perspective corrected scattering regions which can be detected with this equipment. For clarity, the helium chamber is not shown.

fast histogramming memory controller with 64 Mbytes of VME-based memory, a time frame generator and a multi-channel scaler (Helsby, 1993). The latter was configured to collect calibration data from multiple inputs (*i.e.* ion chamber readings, temperature, *etc.*). A stand-alone time-to-amplitude converter system (Helsby *et al.*, 1994) was used to digitize the analogue detector data suitable for input to the histogramming memory.

The data-acquisition software was written in C using object-oriented principles (Ackroyd *et al.*, 1994). Each hardware module was described by a separate piece of software containing its own functions and data, thus allowing a flexible configuration of the system at run-time for different hardware systems.

Deformations were introduced to non-standard dumbbell-shaped specimens using a Polymer Laboratories Minimat with remote microprocessor control. An extension rate of  $1 \text{ mm min}^{-1}$  was used on samples with a ligament radius of 15 mm and a ligament which was 10 mm at its thinnest. The tensile samples had a non-uniform cross section to ensure that they yielded in the beam.

### 3. Results

Static experiments showed that when using a 2 mm thick low-density polyethylene (LDPE) sample, both detectors were heavily saturated with respect to the count rate. In order to reduce this, the beam intensity was reduced to 50% by closing the last two horizontal slit sets before the sample. Even in this situation the WAD pattern had to be attenuated by a factor of  $10^3$  (0.5 mm thick aluminium) and the SAD detector by a factor of 80. However, a large part of this intensity originates from air scatter. The attenuation could be reduced to factors of 30 and 500 for the small- and wide-angle detectors, respectively, if the helium chamber with thin Mylar windows is inserted. This would improve the signal-to-noise ratio by a factor of three.

The number of frames that could be collected in a single run is 20 ( $512 \times 512$  pixels) for both the SAD and the WAD detector. The limit is imposed by the number of memory modules available in the CAMAC system. The intrinsic software limit is 1024 frames. These limitations have prevented the collection of any data with sub-second time resolution since this would require a larger number of frames, but there is no real physical limitation apart from the data rate that the detectors can handle.

Test experiments were performed on high-density polyethylene (HDPE) (Figs. 2 and 3). A piece of this material was placed in a miniature tensile tester (Minimat by Polymer Laboratories, Loughborough) which was mounted on the beamline. Parallel-plate ion chambers were positioned in front of and behind the sample in order to monitor the intensity of the direct and transmitted beam. The outputs of these ion chambers, together with a signal proportional to the force exerted on the sample by the tensile tester, were interfaced to the station computer and sampled as a function

of the frame numbers. Data were collected in a series of 20 time frames with a length of 15 s each. Dead time between the time frames was set to 10  $\mu\text{s}$ .

Prior to the deformation, the HDPE samples exhibited a wide-angle diffraction pattern (Fig. 3) consisting of Debye-Scherrer rings corresponding to the orthorhombic unit cell of polyethylene. The two strong reflections can be indexed as the (110) and (200). The presence of the higher order reflections indicates that the samples were well ordered. The corresponding SAXS pattern (Fig. 2) consisted of a single ring indicating an isotropic distribution of lamellae of a well defined long period ( $d \approx 250 \text{ \AA}$ ).

Under the application of stress, the (110) and (200) reflections began to transform into arcs, indicating that the chains of the molecules were becoming oriented parallel to the tensile axis. Eventually sharp spots were attained, indicating that the samples had become highly oriented with only the equatorial (110) and (200) reflections remaining. In this experiment, the other reflections are not detected since they are on the meridional axis which falls outside the region that can be detected with this detector configuration. To observe these reflections the sample has to be rotated by  $90^\circ$ . The corresponding small-angle patterns also changed considerably. At low strains the isotropic diffraction ring, due to the lamellar stacking of the polyethylene, transforms into a pattern consisting of intense equatorial streaks which are associated with the formation of microvoids accompanying the drawing process. Although the data relating to the long lamellar period were quickly dominated by the scattering due to these voids, information pertaining to the deformation of the samples can still be obtained, and revealed that the voiding process occurred within these samples at strains of less than 5%.

Another interesting feature was observed during the deformation of these samples at intermediate sample strains. Extra reflections were observed on either side of the (110) and (200) reflections. These are indicative of the stress-induced martensitic transformation (Steidl & Pelzbauer, 1972; Young & Bowden, 1974; Hay & Keller, 1970). This transformation involves a change in the crystals from the orthorhombic to the monoclinic unit cell (Hay & Keller, 1970). The four principal modes whereby this transformation can occur have been outlined (Bevis & Crellin, 1971). Previous studies have indicated that this monoclinic form of polyethylene may be unstable and present under stress (Lin & Argonne, 1994), a result which was deduced from the observation that when deformed single crystals of polyethylene were allowed to relax, the reflections due to the monoclinic cell disappeared. This hypothesis has thus been confirmed with these experiments, which have shown conclusively that the monoclinic phase is indeed only retained while the samples are under stress. We believe that this is the first real-time study showing this martensitic transition occurring. It is clear that with further experiments using this experimental set-up, one will be able to provide information relating to this transformation previously not attainable, such as:

(i) the strain at which the martensitic transformation begins to occur,

(ii) the persistence of the monoclinic unit cell with strain, and

(iii) the time scale of the transformation from monoclinic back to orthorhombic upon the removal of stress.

The results of these experiments will be reported elsewhere.

The time resolution that can be achieved with this equipment is still limited by the data rate that the detector systems can handle, as will be clear from the large attenuation factors necessary not to exceed the maximum count rate of the detectors. This is a commonly encountered problem when dealing with synchrotron beamlines. Owing to the fact that the WAD detector is not spherical, the diffraction rings will be distorted to an elliptical form. In order to obtain

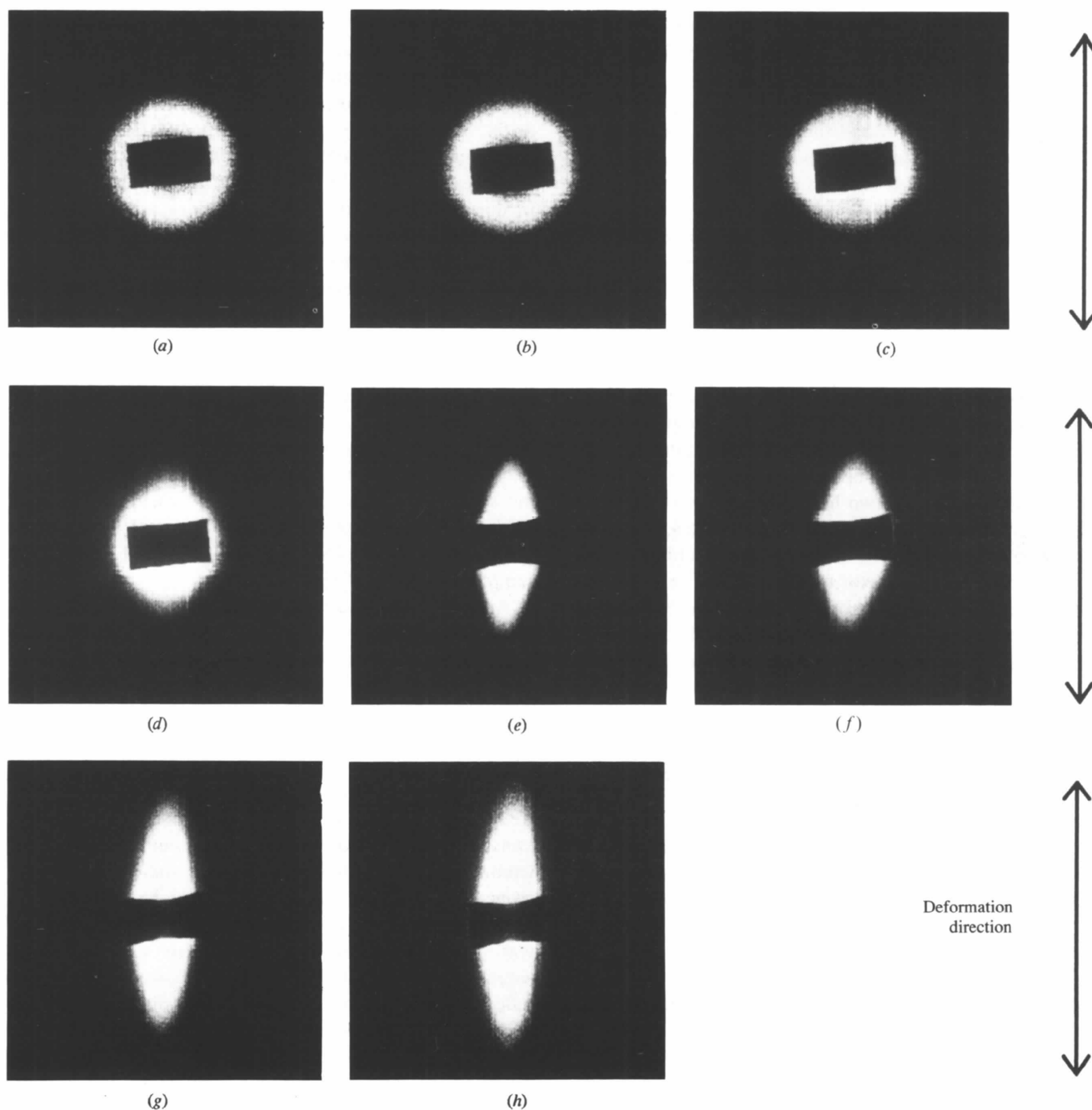


**Figure 2**

(a)–(h) Small-angle fibre diffraction patterns of high-density polyethylene deformed by tensile stress. The patterns are arranged in order of increasing tensile stress. The isotropic diffraction ring due to the lamellar stacking of the molecules is observed in the diffraction pattern of the undeformed material (a). When tensile stress is applied, the low-angle scattering pattern becomes dominated by equatorial diffraction intensity due to the formation of microvoids. The vertical arrows at the end of each row show the deformation direction.

accurate spatial information, one has to correct for this artefact by applying trigonometric corrections to the diffraction pattern. This, however, is outside the remit of this paper and, moreover, of limited interest as this equipment was assembled mainly to establish time correlations between

the changes in the WAD and SAD part of the diffraction pattern. Accurate spatial information in the WAD region is better obtained with the help of either X-ray film or image-plate detectors which have an additional advantage in that they do not suffer from the distortions due to the finite

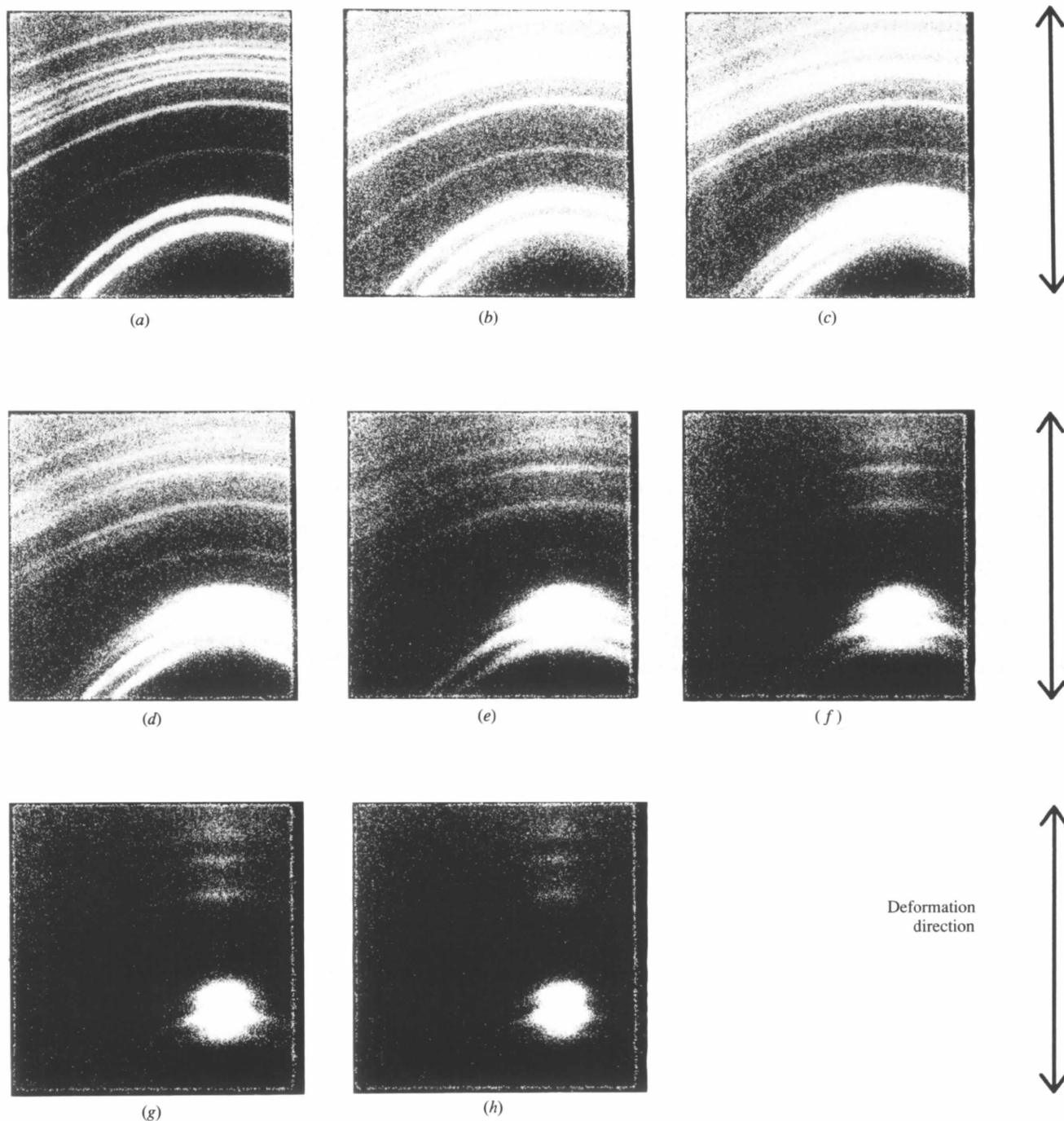


**Figure 3**

(a)–(h) Wide-angle fibre diffraction patterns of high-density polyethylene deformed by tensile stress. The panel numbers correspond to the small-angle diffraction patterns shown in Fig. 2. The strong isotropic scattering rings of the undeformed material (a) can be attributed to the (110) and (200) reflections of the orthorhombic phase. Under the application of stress, the isotropic rings transform into arcs which are centred on the equatorial axis. At intermediate sample strains extra reflections appear on either side of the equatorial diffraction arcs. These are indicative of the transformation from the orthorhombic to the monoclinic phase. The vertical arrows at the end of each row show the deformation direction. The strain field in the sample was not uniform and the local strain was not measured, the yield point occurred between frames 3 and 4.

intrinsic detection depth, a problem encountered when using gas-filled proportional counters.

An interesting fact worth noting is that we were able to collect a diffraction pattern of a single Kevlar fibre (14  $\mu\text{m}$  diameter) in 30 s (sample parallel to the X-ray beam). This was with the attenuation factors mentioned before. Thus, this technique is still basically limited by the data rate that the present generation of imaging detectors can handle, and not by the synchrotron radiation source.

#### 4. Conclusions

We have described a new set-up for simultaneous wide- and small-angle diffraction which is likely to prove a useful tool in establishing the time correlations between changes in the smaller scale structures compared with changes in the larger aggregates that contain the smaller sub-units, when rapid deformations or other morphological changes are applied to samples. The accuracy of measurements of features of the WAD pattern is acceptable when care is taken to position the WAD detector at an angle with respect to the direct beam, so that smearing of diffraction peaks due to the intrinsic depth of the detectors is minimized.

In addition, the deformation of polyethylene occurs by a variety of modes which often involve a combination of chain slip, twinning and the martensitic transformation (Kiho, Peterlin & Geil, 1965). However, the exact interaction between these different deformation modes, and the order in which they occur, is still unclear as previous experiments have had to be performed by post-mortem analysis of deformed samples. Further experiments using this camera will lead to a more complete understanding of the deformation process in semi-crystalline polymers, such as high-density polyethylene.

We would like to thank our colleagues at Daresbury for their help, especially Liz Towns-Andrews for suggesting the experiments, Brian Parker and John Howson for their help with the detector systems, and Dave Bouch and Paul Hindley for their fast response to our engineering needs. Professor R. J. Young is thanked for lending us his tensile tester and suggesting the martensitic transformation in polyethylene.

#### References

- Ackroyd, K. S., Campbell, J. W., Dean, C. E., Enderby, M., Gregory, C. M., Hayes, M. A., Hughes, E. A., Kinder, S. H., Kirkman, I. W., Mant, G. R., Miller, M. C., Milne, G. J., Ramsdale, C. A., Stephenson, P. C. & Pantos, E. (1994). *J. Synchrotron Rad.* **1**, 63–68.
- Bark, M., Schulze, C. & Zachmann, H. (1990). *Polym. Prep. Am. Chem. Soc. Div. Polym. Chem.* **31**(2), 106–107.
- Bevis, M. & Crellin, E. B. (1971). *Polymer*, **12**, 666–684.
- Bras, W., Derbyshire, G. E., Ryan, A. J., Mant, G. R., Manning, P., Cameron, R. E. & Mormann, W. (1993). *J. Phys. (Paris)*, **3**(8), 447–450.
- Hall, C. J. & Lewis, R. A. (1994). *Nucl. Instrum. Methods Phys. Res. A*, **348**, 627–630.
- Hay, I. L. & Keller, A. (1970). *J. Polym. Sci.* **C30**, 289–293.
- Helsby, W. I. (1993). Daresbury Technical Manuals Nos. EC740 and EC738. Daresbury Laboratory, Warrington, UK.
- Helsby, W. I., Hall, C. J., Jones, A. O., Lewis, R. A., Parker, B., Sumner, I. & Berry, A. (1994). *Nucl. Instrum. Methods Phys. Res. A*. Submitted. Daresbury Preprint DL/CSE/P24E.
- Kiho, K., Peterlin, A. & Geil, P. H. (1965). *J. Polym. Sci.* **B3**, 157–160.
- Lewis, R. A., Sumner, I., Berry, A., Bordas, J., Gabriel, A., Mant, G. R., Parker, B., Roberts, K. & Worgan, J. (1988). *Nucl. Instrum. Methods A*, **273**, 773–779.
- Lin, L. & Argonne, A. S. (1994). *J. Mater. Sci.* **29**, 294–323.
- Mant, G. R. (1994). Private communication.
- Steidl, J. & Pelzbauer, Z. (1972). *J. Polym. Sci.* **C38**, 345–356.
- Young, R. J. & Bowden, P. B. (1974). *Philos. Mag.* **29**, 1061–1073.